International Journal of Nanomedicine

Dovepress
open access to scientific and medical research

Open Access Full Text Article

ORIGINAL RESEARCH

A polyethylenimine-modified carboxyl-poly(styrene/acrylamide) copolymer nanosphere for co-delivering of CpG and TGF-β receptor I inhibitor with remarkable additive tumor regression effect against liver cancer in mice

This article was published in the following Dove Press journal:
International Journal of Nanomedicine
13 December 2016
Number of times this article has been viewed

Shuyan Liang*
Jun Hu*
Yuanyuan Xie
Qing Zhou
Yanhong Zhu
Xiangliang Yang

National Engineering Research Center for Nanomedicine, College of Life Science and Technology, Huazhong University of Science and Technology, Wuhan, People's Republic of China

*These authors contributed equally to this work

Abstract: Cancer immunotherapy based on nanodelivery systems has shown potential for treatment of various malignancies, owing to the benefits of tumor targeting of nanoparticles. However, induction of a potent T-cell immune response against tumors still remains a challenge. In this study, polyethylenimine-modified carboxyl-styrene/acrylamide (PS) copolymer nanospheres were developed as a delivery system of unmethylated cytosine-phosphate-guanine (CpG) oligodeoxynucleotides and transforming growth factor-beta (TGF-β) receptor I inhibitors for cancer immunotherapy. TGF-β receptor I inhibitors (LY2157299, LY) were encapsulated to the PS via hydrophobic interaction, while CpG oligodeoxynucleotides were loaded onto the PS through electrostatic interaction. Compared to the control group, tumor inhibition in the PS-LY/CpG group was up to 99.7% without noticeable toxicity. The tumor regression may be attributed to T-cell activation and amplification in mouse models. The results highlight the additive effect of CpG and TGF-β receptor I inhibitors co-delivered in cancer immunotherapy.

Keywords: CpG, TGF-β receptor I inhibitor, Pst-AAm copolymer nanosphere, immunotherapy

Introduction

Immunotherapy has shown the potential to become an essential component of a successful antitumor treatment.[1] The generation of an antitumor immune response at the location of tumor is important for tumor regression.[2] Nanoparticles have the intrinsic advantages of accumulating into tumor by the enhanced permeability and retention effect.[3,4] In this respect, the design and synthesis of nanomaterials loading immunotherapy drugs have been of great interest for cancer immunotherapy.

Unmethylated cytosine-phosphate-guanine (CpG) oligodeoxynucleotide characterized by bacterial and viral DNA, which induces cytokine production through recognition by Toll-like receptor 9, activates innate and acquired immune responses.[5] The inflammatory cytokines induced by CpG can elicit $CD8^+$ T-cell responses.[6,7] Meanwhile, $CD8^+$ T-cell immune response is the major cell-mediated immune response for antitumor effects.[8–10] Therefore, CpG can be used as a potential immunotherapy agent against malignancies.

Transforming growth factor-beta (TGF-β) is one of the most influential cytokines among a number of factors expressed in tumor stroma.[11,12] Expression of TGF-β in human cancers correlates with cancer progression and poor clinical outcome.[13] TGF-β regulates the progression of cancer through its effects on tumor microenvironment by orchestrating a favorable microenvironment for tumor cell growth.[11,14] Inhibitors for

Correspondence: Yanhong Zhu; Xiangliang Yang
National Engineering Research Center for Nanomedicine, College of Life Science and Technology, Huazhong University of Science and Technology, 1037 Luoyu Road, Wuhan 430074, Hubei, People's Republic of China
Tel +86 27 8779 2147
Fax +86 27 8779 2234
Email yhzhu@hust.edu.cn; nanomedicine@hust.edu.cn

submit your manuscript | www.dovepress.com
Dovepress
http://dx.doi.org/10.2147/IJN.S122047

inhibiting TGF-β signal pathway have recently been shown to prevent the growth and metastasis of certain cancers.[15] Therefore, TGF-β is thought to be an important target for cancer therapy. Moreover, CD8 T cytotoxicity could be suppressed by TGF-β signals in vivo.[16] Therefore, inhibition of TGF-β signal pathway combined with promoted CD8 T cytotoxicity might achieve synergistic antitumor effects.

In the present study, the antitumor effects of CpG that induce CD8 T cytotoxicity combined with TGF-β receptor I inhibitor were investigated. TGF-β receptor inhibitor I LY2157299 (LY) is one of the TGF-β receptor inhibitors under preclinical and clinical trials.[13,17,18] Polyethylenimine (PEI) with high positive charge was used for gene delivery frequently.[19] To co-deliver hydrophilic CpG with negative charge and hydrophobic LY at the same time, polyethylenimine-modified carboxyl-styrene/acrylamide (PS) copolymer nanospheres, a unique structure characterized by hydrophobic cavities and hydrophilic positive surface, was used as the drug delivery system. The hydrophobic LY was encapsulated in the cavities of PS nanoparticle via hydrophobic interaction, while CpG was loaded onto the PS nanoparticle through electrostatic interaction. The present findings strongly suggest that a combination of low-dose small molecule LY and CpG in a nanocarrier is a promising way to treat intractable cancers.

Materials and methods

Materials

CpG1826 was from Sangon Biotech Co., Ltd (Shanghai, People's Republic of China). TGF-β receptor I inhibitor LY2157299 was from Shengda Pharmaceutical Co. (Shenzhen, People's Republic of China). PEI (MW 25 kD) was from Sigma-Aldrich Co. (St Louis, MO, USA). Antibodies were from BioLegend (San Diego, CA, USA). Other chemicals and reagents purchased from commercial suppliers were of analytical grade, unless otherwise noted.

All cell lines used in the study were preserved in our lab and cultured in Dulbecco's Modified Eagle's Medium (containing 10% fetal bovine serum [FBS]) at 37°C in a 5% CO_2 incubator. The cell lines were purchased from the China Center for Type Culture Collection and preserved in our lab. Because the authors did not get the cell lines directly from a human, use of the cell lines did not need to be approved by the ethics committee (Ethics Committee of Tongji Medical College, Huazhong University of Science and Technology).

Construction of PEI-modified Pst-AAm copolymer nanospheres

Poly(styrene/acrylamide) (Pst-AAm) with hydrophobic cavities were synthesized through a modified emulsion-free polymerization method in aqueous solution as reported previously.[20–28] Typically, 10 g of styrene was added into a three-neck flask containing 80 mL of de-oxygen water at 75°C under vigorous stirring. When styrene was homogeneously dispersed, 2.5 g of recrystallized acrylamide and 0.25 g of potassium persulfate dissolved in 10 mL of de-ionized water were sequentially added. The reaction was maintained for 6 hours under continuous nitrogen bubbling. The products were collected after filtration followed by a dialysis process to remove large particles and unreacted small molecules, respectively. During this procedure, water-soluble initiator first induces the polymerization of acrylamide providing long-chain polymers, which tend to form micelle-like structure. Subsequently, water-insoluble styrene monomers diffuse into the hydrophobic inner part of the micelles to participate in the polymerization. As a consequence, Pst-AAm copolymer nanospheres are obtained with a hydrophilic outer surface and hydrophobic inner hollow cavities. Subsequent PEI conjugation was performed via carbodiimide cross-linking reaction followed by carboxyl modification of the synthesized Pst-AAm copolymer nanospheres. Successively washed with 0.5 M NaCl solution and de-ionized water to remove any free PEI molecules, the positively modified Pst-AAm copolymer nanospheres were re-dispersed in 1 mL phosphate-buffered saline (PBS) (pH =7.2) and incubated with 10 mg of N-hydroxysuccinimide-polyethylene glycol (PEG) 2,000 overnight under gentle shaking. Surplus PEG was removed by washing three times with de-ionized water, and then PS nanospheres were obtained.

Preparation of PS-LY/CpG nanoparticle

In total, 20 μL (1 mg/mL) of LY (dissolved in chloroform) was added slowly into 3 mL diluted PS water solution in a dropwise manner under stirring, and then spinned to obtain PS-LY nanoparticle. After washing, the deposit of PS-LY nanoparticle was resuspended in 1 mL distilled water and mixed with 2 optical density CpG under vortexing. After spinning, the PS-LY/CpG nanoparticles were obtained. The supernatants were collected to analyze drug-loading capacity.

Characterization of the nanoparticle

The size and the morphology of PS nanosphere and PS-LY/CpG nanoparticle were characterized through transmission electron microscopy (JEM-2010; JEOL, Tokyo, Japan). The hydrodynamic diameter and the zeta potential were measured with a Malvern Zetasizer Nano ZS in water (Malvern, Worcestershire, UK). The drug loading of LY was detected via high purity liquid chromatography system (Agilent HP-1100; Agilent Technologies, Santa Clara, CA, USA). Chromatographic separation was performed on a column of Agilent TC-C18 (4.6×250 mm,

5 μm particle size) at room temperature with the mobile phase consisting of a mixture of acetonitrile-water (50:50). CpG was detected through ultraviolet spectroscopy at 260 nm.

Cell toxicity analysis

Normal human embryonic kidney 293 cell line (HEK293 cell) was used for cytotoxicity analysis through the 3-(4,5-dimethylthiazol-2yl)-2,5-diphenyltetrazolium bromide (MTT) method. After cells were treated with the materials, 20 μL of MTT (5 mg/mL) was added to each well. Then, formazan crystals were solubilized with 150 μL of dimethyl sulfoxide 4 hours later. The absorbance at 490 nm of each well was used to determine the relative cell viability.

Xenograft studies

All animal studies were approved by the Animal Experimentation Ethics Committee of College of Life Science and Technology, Huazhong University of Science and Technology. The procedures abided by the animal care guidelines of the Science and Technology Department of Hubei Province.

BALB/c mice (male, 4–6 weeks) were purchased from Hubei Provincial Center for Disease and Prevention, People's Republic of China. In total, 6×10^5 liver cancer H22 cells were inoculated in a BALB/c mouse to establish the subcutaneous tumor model. Antitumor effects of the nanoparticle were evaluated in vivo. Four groups were intratumorally injected with PBS, PS-LY, PS-CpG, and PS-LY/CpG, respectively, on day 8 after tumor cells were inoculated. Drugs were administered six times in 2-day intervals. Tumor sizes were serially measured with calipers every 2 days.

Tumor volumes were calculated according to the following formula: tumor volume = (tumor length × tumor width^2)/2.[29] Sera were collected and stored at –20°C in 100 μL aliquots. Spleen cells were harvested and rinsed in PBS for fluorescence activating cell sorter analysis. Xenografts and spleen tissues were fixed in 4% paraformaldehyde, followed by embedding in paraffin.

Flow cytometry analysis

Antibodies anti-CD3 and CD8 were incubated with cells in PBS containing 1% FBS for 30 minutes at 4°C. After washing, the cells were analyzed through flow cytometry. CD8-positive T-cell populations were described as $CD3^+/CD8^+$ T-cells.

Histological analysis

Spleen was sliced up for immunohistochemistry analysis.[30] According to standard techniques, the tissues were fixed with formalin and then embedded with paraffin before being sectioned. The paraffin sections were dewaxed before staining. Slides were incubated with monoclonal antibodies and detected by streptavidin-peroxidase method. $CD3^+/CD8^+$ T-cells were used to identify CD8-positive T-cells. To detect tumor fibrosis, the tumor tissues in different groups were sliced up for Masson's trichrome staining according to the report.[31]

Statistics analysis

All data were calculated using Prism 5.0 software (GraphPad, San Diego, CA, USA). Statistical differences were determined according to Student's *t* test. A *P*-value of less than 0.05 was considered to be statistically significant.

Results and discussion

Characterization of nanoparticles

Scheme 1 presents an illustration of the synthesis process of PS-LY/CpG nanoparticle.

From the transmission electron microscope images, the average size of PS nanoparticles was about 230 nm (Figure 1A). After loading with LY and CpG, the average size of PS-LY/CpG was about 300 nm. Compared to PS and PS-LY, the rougher surface of PS-LY/CpG was observed when CpG were loaded onto the particle. The results of DLS showed that the hydrodynamic diameters of PS, PS-LY, and PS-LY/CpG were about 237.2±12.5 nm, 261.4±11.0 nm, and 331.2±17.2 nm, respectively (Figure 1B). The successful binding of CpG to PS-LY was confirmed by a surface charge reversal (the zeta potential of PS, PS-LY, and PS-LY/CpG was 37.9±0.8 mV, 39.9±0.6 mV, and –25.5±0.4 mV, respectively). The drug loading of LY and CpG was 18% and 2.3%, respectively. LY was released up to 10.6% in 24 hours, followed by continuous steady release in vitro (Figure S1).

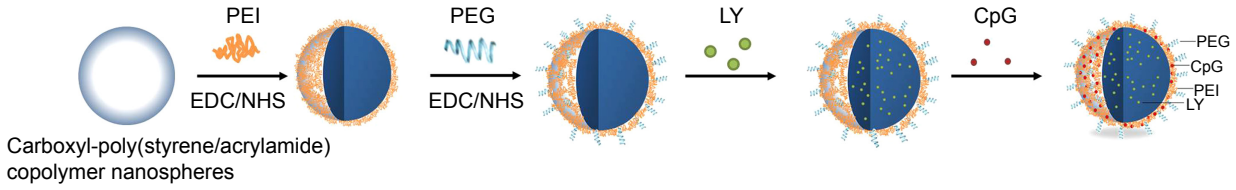

Scheme 1 An illustration of the synthesis process of PS-LY/CpG nanoparticle.
Abbreviations: PS, polyethylenimine-modified carboxyl-styrene/acrylamide; LY, LY215729; CpG, cytosine-phosphate-guanine; PEI, polyethylenimine; PEG, polyethylene glycol; EDC, 1-ethyl-3-(3-dimethylaminopropyl)carbodiimide hydrochloride; NHS, N-hydroxysuccinimide.

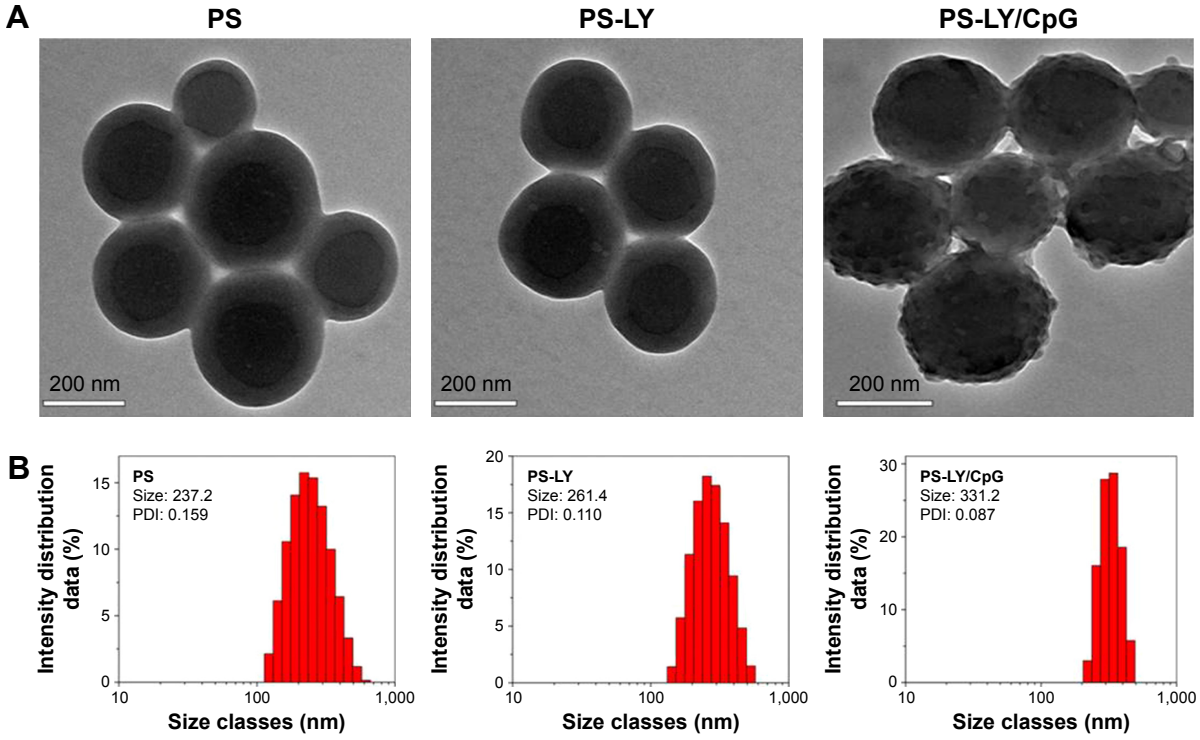

Figure 1 Sizes and morphologies of PS, PS-LY, and PS-LY/CpG under transmission electron microscope (**A**). Diameters of dynamic light scattering (237.2±12.5 nm, 261.4±11.0 nm, and 331.2±17.2 nm) (**B**).
Abbreviations: PS, polyethylenimine-modified carboxyl-styrene/acrylamide; LY, LY215729; CpG, cytosine-phosphate-guanine; PDI, polydispersity index.

Biocompatibility studies

PS-LY/CpG did not affect the metabolic activity in a time-dependent manner when 20 μg/mL (PS concentration) was added to HEK293 cells (Figure 2A). The biocompatibility in vivo was evaluated too. The body weights of mice did not change significantly after administration of PS-LY/CpG (Figure 2B). A variety of nanodelivery systems have been utilized in an attempt to reduce the cellular toxicity of CpG Oligodeoxynucleotids and achieve optimal stability.[32–34] In this study, the surface of PS was modified by PEG, which

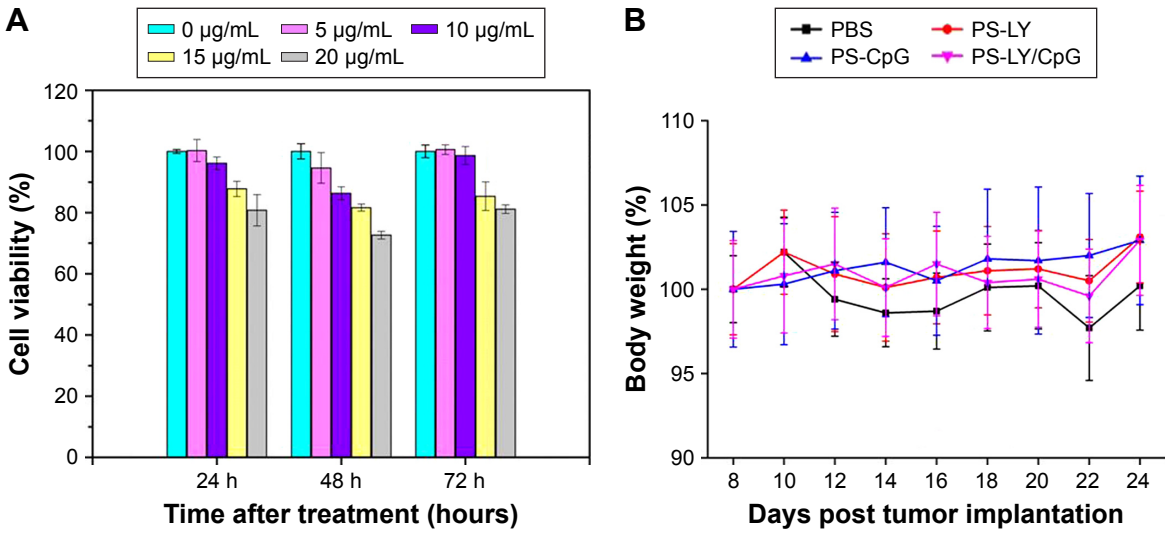

Figure 2 Biocompatibility of PS-LY/CpG.
Notes: In total, ≥80% cells maintaining viability were treated with PS-LY/CpG at different concentrations (**A**). No significant change in body weight of different groups was observed (**B**) (n=6).
Abbreviations: PS, polyethylenimine-modified carboxyl-styrene/acrylamide; LY, LY215729; CpG, cytosine-phosphate-guanine; PBS, phosphate-buffered saline.

elicited its good compatibility. CpG carried by the PS appeared to limit its toxicity.

Antitumor effects of PS-LY/CpG nanoparticle

Significantly enhanced antitumor effects of PS-LY/CpG were verified in vivo. Figure 3 shows the tumor volume and weight changes after the mice were treated with PS-LY, PS-CpG, or PS-LY/CpG. LY at a dose of 1 mg/kg and CpG at a dose of 0.33 mg/kg were administered to the animals. PS-LY alone could not significantly inhibit tumor growth, whereas PS-LY/CpG treatment led to a drastic inhibition of tumor growth. Compared to the PBS group, tumor inhibition rate was up to 99.7% in the PS-LY/CpG group. Based on the tumor volume and weight results, PS-LY/CpG enhanced antitumor effects compared to PS-LY or PS-CpG, which revealed the additive effects of CpG and LY.

Because of the instability and toxicity of CpG in blood, therapeutic activity of CpG alone was observed after only intratumoral administration of CpG.[35] CpG nanoparticles induced stronger immunotherapy effects than free CpG administered via intravenous injection due to preferentially tumor-targeting ability of nanoparticle.[36] Compared to free CpG, CpG nanoparticles can significantly enhance the survival rate of lung cancer.[34] A variety of studies of CpG against cancer as adjuvant or immunotherapy agent delivered by nanodelivery were reported,[37] while it is still highly demanding to develop a simple and cost-efficient approach to applicability of CpG ODNs in biological studies and even in clinical trials. Co-delivery of CpG and LY to tumor for immunotherapy is rarely reported.

Analysis of immune cells

In this study, T-cell immune stimulatory activity and replication were exhibited in the PS-LY/CpG group. Based on the flow cytometry analysis results (Figure 4), total T-cell numbers were significantly increased after the mice were treated with PS-CpG or PS-LY/CpG. Although increase in absolute number of the subtype $CD3^+/CD8^+$ T-cell in the PS-LY/CpG group did not reach statistical significance (P=0.51), it was noticeable compared with that in the PBS group. Our results agree with the report that CpG enhanced

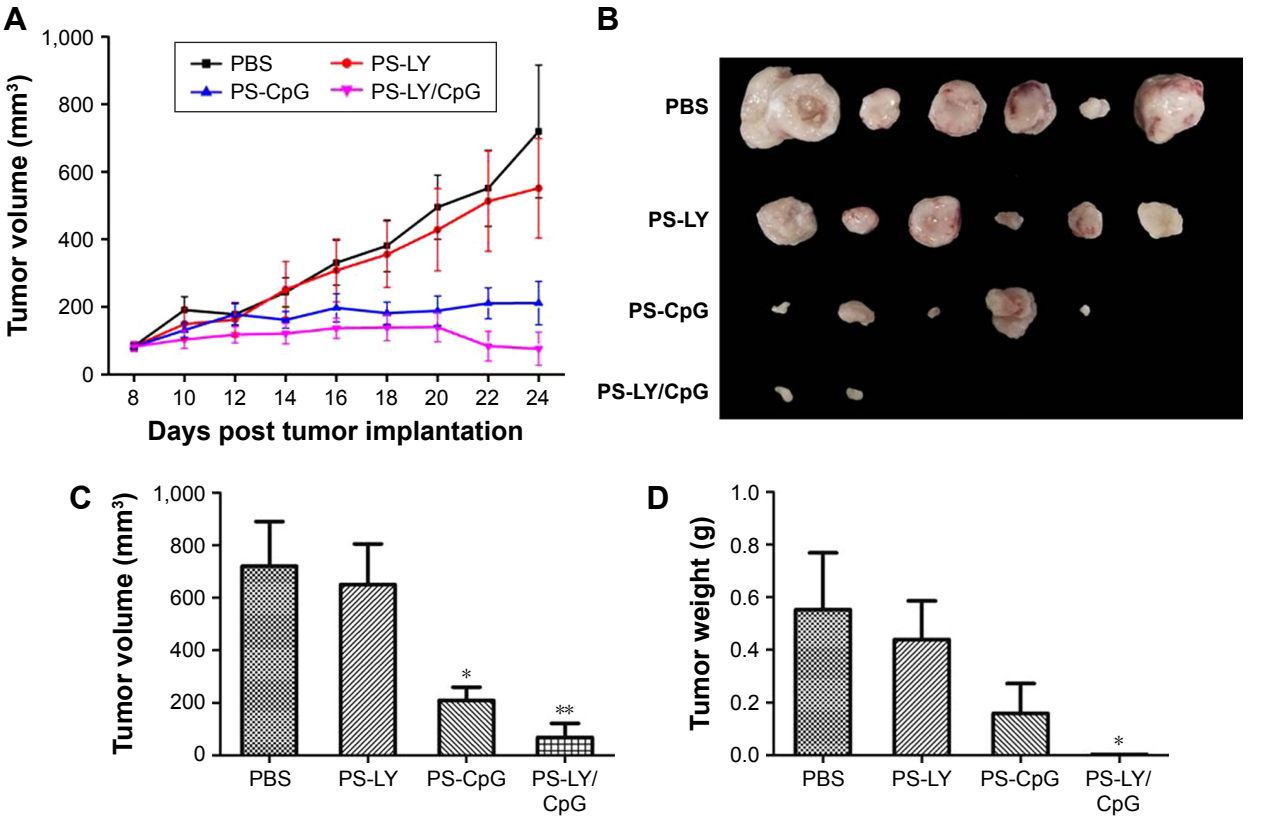

Figure 3 Antitumor effects of PS-LY/CpG.

Notes: Drugs were administered six times at 2-day intervals. Tumor sizes were serially measured with calipers every 2 days. Changes of tumor volume after treatments (**A**); photograph of the tumors extracted from the mice bearing H22 tumors at 24 days post inoculation of tumor cells (**B**); tumor volume and weight when mice were sacrificed (**C** and **D**); n=6. *P<0.05; **P<0.01.

Abbreviations: PS, polyethylenimine-modified carboxyl-styrene/acrylamide; LY, LY215729; CpG, cytosine-phosphate-guanine; PBS, phosphate-buffered saline.

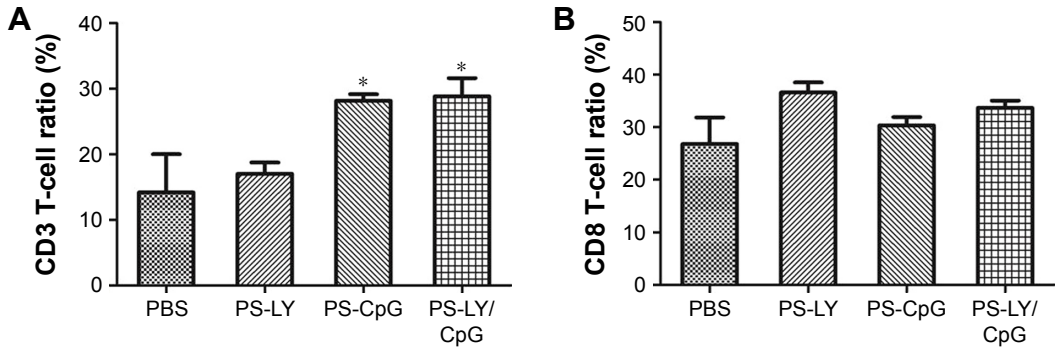

Figure 4 Changes of spleen T-cell number treated with PS-LY/CpG through flow cytometry analysis.
Notes: Total T-cell proliferation in spleen after treatments (**A**). $CD8^+$ T-cell number increased in the PS-CpG and PS-LY/CpG groups compared to the PBS group (**B**). *$P<0.05$ compared to PBS group.
Abbreviations: PS, polyethylenimine-modified carboxyl-styrene/acrylamide; LY, LY215729; CpG, cytosine-phosphate-guanine; PBS, phosphate-buffered saline.

Th1 immune responses, and formulations containing them were against certain types of cancer.[35] In the present study, PS-LY/CpG could lead to antitumor effects by inducing the $CD8^+$ T-cell response. $CD8^+$ T-cell immune responses are the major cell-mediated immune responses leading to potent antitumor effects.[8,38]

Histological analysis

The results of tumor tissue immunohistochemistry were consistent with those of flow cytometry analysis. The $CD8^+$ T-cell number was higher in the PS-CpG group and PS-LY/CpG group than that in the PBS group (Figure 5). $CD8^+$ T-cell responses were required to reject the tumor in the tumor

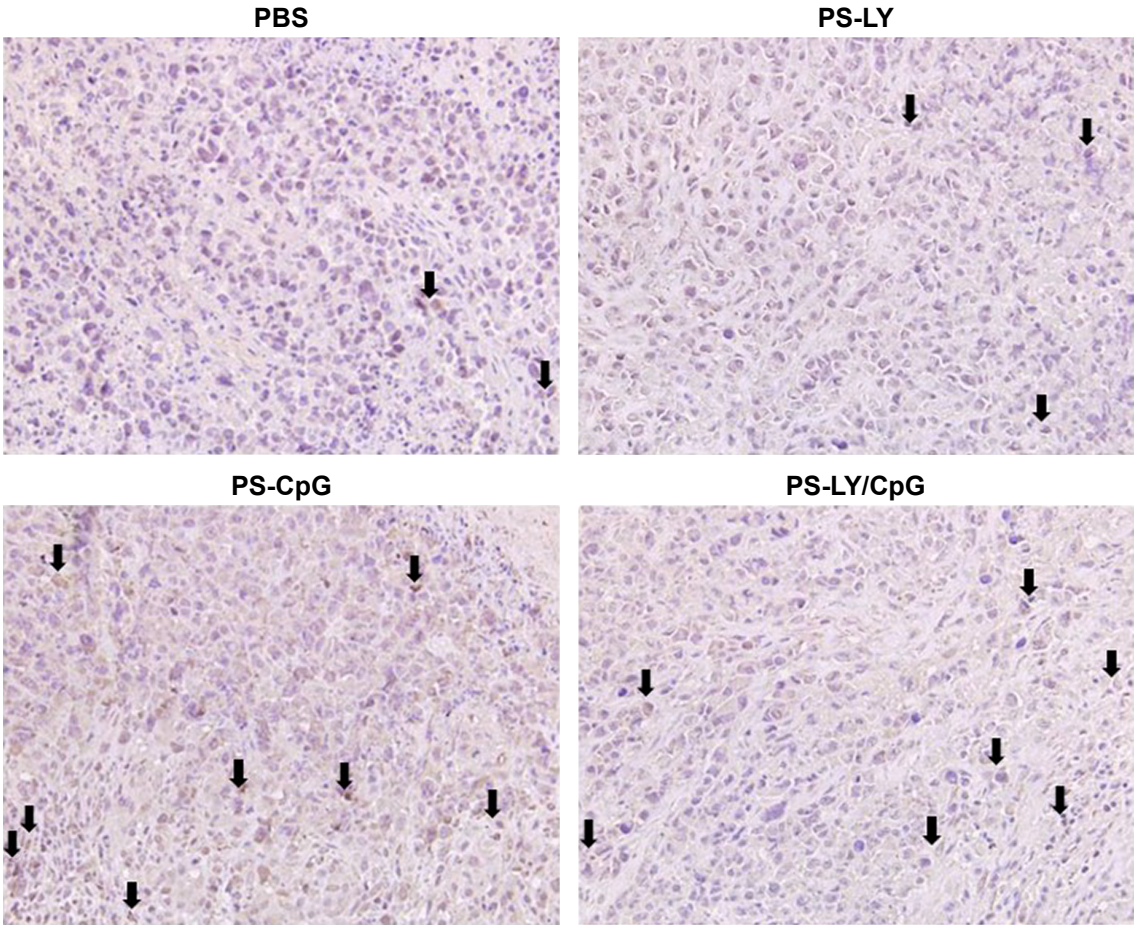

Figure 5 Immunohistochemistry staining of $CD8^+$ T-cells in tumor tissues.
Note: $CD8^+$ T-cells (arrows) increased in the PS-CpG group and the PS-LY/CpG group through immunohistochemistry analysis.
Abbreviations: PS, polyethylenimine-modified carboxyl-styrene/acrylamide; LY, LY215729; CpG, cytosine-phosphate-guanine; PBS, phosphate-buffered saline.

immunotherapy.[38] In this study, $CD8^+$ T-cells customized to the tumor site, which induced the cytotoxic response to control the growth of tumor in vivo.

After Masson's trichrome staining, the collagen fibers were stained blue. Collagen fibers were rich in the tumor tissue of the PBS group (Figure S2), whereas their number decreased in the PS-LY group. Antitumor effects of LY in the study were consistent with those of the reports.[39,40] Phase I safety and dose-finding clinical trials with LY2157299 have shown that it is well tolerated.[41–43] Efficacy studies using an intermittent schedule of LY are currently ongoing in patients with hepatocellular carcinoma and multiple myeloma.[13,44] The decrease in the number of collagen fibers in the PS-CpG and PS-LY/CpG groups may be attributed to tumor remission.

Conclusion

In summary, co-delivery of LY and CpG by PS nanospheres showed great physical-chemical properties and antitumor activity. $CD8^+$ T-cell responses may be the potential mechanism for additive antitumor effects. Since immunotherapy plays an important role in cancer therapy, PS-LY/CpG may have great potential in treating liver cancer and other tumors.

Acknowledgments

This work was financially supported by the National Natural Science Foundation of China (81573013) and the grant from National Basic Research Program of China (973 Program, 2012CB932500). We are thankful to the Analysis and Test Center of Huazhong University of Science and Technology.

Disclosure

The authors report no conflicts of interest in this work.

References

1. Mellman I, Coukos G, Dranoff G. Cancer immunotherapy comes of age. *Nature*. 2011;480:480–489.
2. Song L, Yang MC, Knoff J, Sun ZY, Wu TC, Hung CF. Cancer immunotherapy using a potent immunodominant CTL epitope. *Vaccine*. 2014; 32(46):6039–6048.
3. Maeda H, Bharate GY, Daruwalla J. Polymeric drugs for efficient tumor-targeted drug delivery based on EPR-effect. *Eur J Pharm Biopharm*. 2009;71:409–419.
4. Torchilin V. Tumor delivery of macromolecular drugs based on the EPR effect. *Adv Drug Deliv Rev*. 2011;63:131–135.
5. Krieg AM. Antiinfective applications of Toll-like receptor 9 agonists. *Proc Am Thorac Soc*. 2007;4(3):289–294.
6. Askew D, Chu RS, Krieg AM, Harding CV. CpG DNA induces maturation of dendritic cells with distinct effects on nascent and recycling MHCII antigen-processing mechanisms. *J Immunol*. 2000;165: 6889–6895.
7. Behboudi S, Chao D, Klenerman P, Austyn J. The effects of DNA containing CpG motif on dendritic cells. *Immunology*. 2000;99:361–366.
8. Antony PA, Piccirillo CA, Akpinarli A, et al. CD8+ T cell immunity against a tumor/self-antigen is augmented by CD4+ T helper cells and hindered by naturally occurring T regulatory cells. *J Immunol*. 2005;174: 2591–2601.
9. Zoglmeier C, Bauer H, Nörenberg D, et al. CpG blocks immunosuppression by myeloid-derived suppressor cells in tumor-bearing mice. *Clin Cancer Res*. 2011;17:1765–1775.
10. Shirota Y, Shirota H, Klinman DM. Intratumoral injection of CpG oligonucleotides induces the differentiation and reduces the immunosuppressive activity of myeloid-derived suppressor cells. *J Immunol*. 2012; 188:1592–1599.
11. Alshaker HA, Matalka KZ. IFN-g, IL-17 and TGF-b involvement in shaping the tumor microenvironment: the significance of modulating such cytokines in treating malignant solid tumors. *Cancer Cell Int*. 2011;11: 33–45.
12. Kano MR, Bae Y, Iwata C, et al. Improvement of cancer-targeting therapy, using nanocarriers for intractable solid tumors by inhibition of TGF-β signaling. *Proc Natl Acad U S A*. 2007;104(9):3460–3465.
13. Oyanagi J, Kojima N, Sato H, et al. Inhibition of transforming growth factor-β signaling potentiates tumor cell invasion into collagen matrix induced by fibroblast-derived hepatocyte growth factor. *Exp Cell Res*. 2014;326:267–279.
14. Giannelli G, Villa E, Lahn M. Transforming growth factor-β as a therapeutic target in hepatocellular carcinoma. *Cancer Res*. 2014;74(7): 1890–1894.
15. Bhola NE, Balko JM, Dugger TC, et al. TGF-β inhibition enhances chemotherapy action against triple-negative breast cancer. *J Clin Invest*. 2013;123(3):1348–1358.
16. Chen ML, Pittet MJ, Gorelik L, et al. Regulatory T cells suppress tumor-specific CD8 T cell cytotoxicity through TGF-β signals in vivo. *Proc Natl Acad Sci U S A*. 2005;102(2):419–424.
17. Wharton K, Derynck R. TGF-β family signaling: novel insights in development and disease. *Development*. 2009;136(22):3691–3697.
18. Bandyopadhyay A, Agyin JK, Wang L, et al. Inhibition of pulmonary and skeletal metastasis by a transforming growth factor-β type I receptor kinase inhibitor. *Cancer Res*. 2006;66:6714–6721.
19. Xie J, Teng L, Yang Z, et al. Polyethylenimine-linoleic acid conjugate for antisense oligonucleotide delivery. *BioMed Res Int*. 2013;2013:1–7.
20. Xie HY, Zuo C, Liu Y, et al. Cell-targeting multifunctional nanospheres with both fluorescence and magnetism. *Small*. 2005;1:506–509.
21. Song EQ, Wang GP, Xie HY, et al. Visual recognition and efficient isolation of apoptotic cells with fluorescent-magnetic-biotargeting multifunctional nanospheres. *Clin Chem*. 2007;53:2177–2185.
22. Xie HY, Xie M, Zhang ZL, et al. Wheat germ agglutinin-modified trifunctional nanospheres for cell recognition. *Bioconjug Chem*. 2007; 18:1749–1755.
23. Hu J, Xie M, Wen CY, et al. A multicomponent recognition and separation system established via fluorescent, magnetic, dual-encoded multifunctional bioprobes. *Biomaterials*. 2011;32:1177–1184.
24. Song EQ, Hu J, Wen CY, et al. Fluorescent-magnetic-biotargeting multifunctional nanobioprobes for detecting and isolating multiple types of tumor cells. *ACS Nano*. 2011;5:761–770.
25. Wen CY, Hu J, Zhang ZL, et al. One-step sensitive detection of Salmonella typhimurium by coupling magnetic capture and fluorescence identification with functional nanospheres. *Anal Chem*. 2013;85(2):1223–1230.
26. Hu J, Wen CY, Zhang ZL, et al. Optically encoded multifunctional nanospheres for one-pot separation and detection of multiplex DNA sequences. *Anal Chem*. 2013;85:11929–11935.
27. Hu J, Wen CY, Zhang ZL, Xie M, Xie HY, Pang DW. Recognition kinetics of biomolecules at the surface of different-sized spheres. *Biophys J*. 2014;107:165–173.
28. Wen CY, Wu LL, Zhang ZL, et al. Quick-response magnetic nanospheres for rapid, efficient capture and sensitive detection of circulating tumor cells. *ACS Nano*. 2014;8:941–949.
29. Qu X, Felder MA, Perez Horta Z, Sondel PM, Rakhmilevich AL. Antitumor effects of anti-CD40/CpG immunotherapy combined with gemcitabine or 5-fluorouracil chemotherapy in the B16 melanoma model. *Int Immunopharmacol*. 2013;17(4):1141–1147.

30. Wang Q, Sachse P, Semmo M, et al. T- and B-cell responses and previous exposure to hepatitis B virus in 'anti-HBc alone' patients. *J Viral Hepat*. 2015;22(12):1068–1078.
31. Han J, Liang H, Yi J, et al. Long-term selenium-deficient diet induces liver damage by altering hepatocyte ultrastructure and MMP1/3 and TIMP1/3 expression in growing rats. *Biol Trace Elem Res*. Epub 2016 Jun 24.
32. Wei M, Chen N, Li J, et al. Polyvalent immunostimulatory nanoagents with self-assembled CpG oligonucleotide-conjugated gold nanoparticles. *Angew Chem Int Ed Engl*. 2012;51:1202–1206.
33. Wilson KD, de Jong SD, Tam YK. Lipid-based delivery of CpG oligonucleotides enhances immunotherapeutic efficacy. *Adv Drug Deliv Rev*. 2009;61:233–242.
34. Kuramoto Y, Nishikawa M, Hyoudou K, Yamashita F, Hashida M. Inhibition of peritoneal dissemination of tumor cells by single dosing of phosphodiester CpG oligonucleotide/cationic liposome complex. *J Control Release*. 2006;115:226–233.
35. Kim DH, Moon C, Oh SS, et al. Liposome-encapsulated CpG enhances antitumor activity accompanying the changing of lymphocyte populations in tumor via intratumoral administration. *Nucleic Acid Ther*. 2015;25(2):95–102.
36. de Titta A, Ballester M, Julier Z, et al. Nanoparticle conjugation of CpG enhances adjuvancy for cellular immunity and memory recall at low dose. *Proc Natl Acad Sci U S A*. 2013;110(49):19902–19907.
37. Buhtoiarov IN, Sondel PM, Wigginton JM, et al. Anti-tumour synergy of cytotoxic chemotherapy and anti-CD40 plus CpG-ODN immunotherapy through repolarization of tumour-associated macrophages. *Immunology*. 2011;132:226–239.
38. Lonsdorf AS, Kuekrek H, Stern BV, Boehm BO, Lehmann PV, Tary-Lehmann M. Intratumor CpG-oligodeoxynucleotide injection induces protective antitumor T cell immunity. *J Immunol*. 2003;171:3941–3946.
39. Bauer JA, Ye F, Marshall CB, et al. RNA interference (RNAi) screening approach identifies agents that enhance paclitaxel activity in breast cancer cells. *Breast Cancer Res*. 2010;12(3):R41.
40. Wang Y, Deng B, Tang W, Liu T, Shen X. TGF-β1 secreted by hepatocellular carcinoma induces the expression of the foxp3 gene and suppresses antitumor immunity in the tumor microenvironment. *Dig Dis Sci*. 2013;58(6):1644–1652.
41. Clarke JM, Hurwitz HI. Understanding and targeting resistance to anti-angiogenic therapies. *J Gastrointest Oncol*. 2013;4(3):253–263.
42. Zhang M, Lahn M, Huber PE. Translating the combination of TGF-β blockade and radiotherapy into clinical development in glioblastoma. *Oncoimmunology*. 2012;1(6):943–945.
43. Maluccio M, Sharma V, Lagman M, et al. Tacrolimus enhances transforming growth factor-β1 expression and promotes tumor progression. *Transplantation*. 2003;76(3):597–602.
44. Hawinkels LJ, Ten Dijke P. Exploring anti-TGF-β therapies in cancer and fibrosis. *Growth Factors*. 2011;29(4):140–152.

Supplementary materials

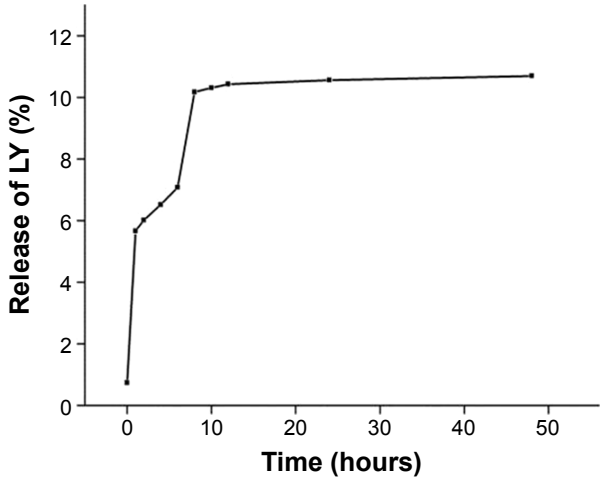

Figure S1 Release of LY.
Note: In total, 10.6% LY was released within 24 hours, after which it was released slowly.
Abbreviation: LY, LY215729.

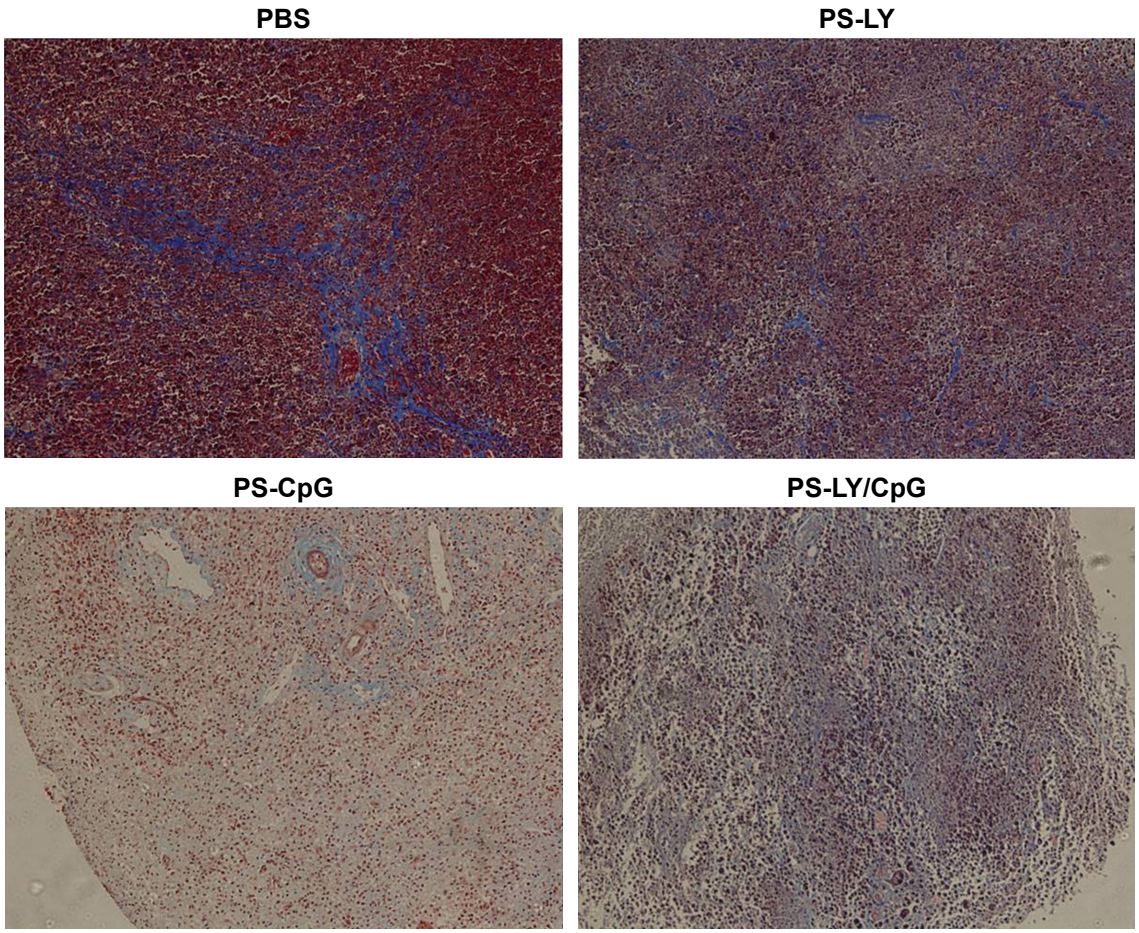

Figure S2 Comparison of Masson's trichrome staining of tumor tissues under different treatments.
Note: Collagen fibers (blue) were rich in the PBS group and poor in other groups.
Abbreviations: PBS, phosphate-buffered saline; PS, polyethylenimine-modified carboxyl-styrene/acrylamide; LY, LY215729; CpG, cytosine-phosphate-guanine.